

# Investigating the Adsorption Behavior and Mechanism of Eu(III) and Au(III) on $\beta$ -cyclodextrin/polyethylenimine Functionalized Waste Paper

**Fenglei Liu**

Shaoxing University

**Shan Hua**

Shaoxing University

**Qingyuan Hu**

Shaoxing University

**Chao Wang**

Shaoxing University

**baowei hu** (✉ [hbw@usx.edu.cn](mailto:hbw@usx.edu.cn))

Shaoxing University

---

## Research Article

**Keywords:** Waste paper,  $\beta$ -CD, Eu(III), Au(III), Adsorption

**Posted Date:** September 21st, 2021

**DOI:** <https://doi.org/10.21203/rs.3.rs-892094/v1>

**License:**   This work is licensed under a Creative Commons Attribution 4.0 International License.

[Read Full License](#)

---

**Version of Record:** A version of this preprint was published at Cellulose on January 29th, 2022. See the published version at <https://doi.org/10.1007/s10570-021-04389-2>.

# Abstract

A bio-adsorbent (DAWP-PEI- $\beta$ -CD) was facilely prepared by introducing polyethylenimine (PEI) and  $\beta$ -cyclodextrin ( $\beta$ -CD) into dialdehyde waste paper (DAWP) via a facile two-step method. Various physicochemical and spectroscopic techniques (FT-IR, XRD, SEM, NMR, XPS) were applied to characterize the structure, morphology and composition of the as-prepared adsorbents. Investigation results showed that the pH values, reaction temperature and contact time played a vital role in uptake of Eu(III) and Au(III). Meanwhile, the adsorption behavior of Eu(III) and Au(III) could be fitted felicitously with the Langmuir and the Pseudo-second-order models, and the saturated adsorption amounts of Eu(III) (pH = 6.0) and Au(III) (pH = 2.0) onto DAWP-PEI- $\beta$ -CD were 424.2 and 241.3 mg/g, respectively. Further advanced spectroscopy analysis revealed that the elimination of Eu(III) was attributed to host-guest inclusion and surface complexation interaction, while adsorption of Au(III) might stem from a combination of electrostatic attraction, chelation, host-guest inclusion and redox interaction. This study demonstrated that DAWP-PEI- $\beta$ -CD was a promising environmental functional material to separation and enrichment of Eu(III) and Au(III) from contaminated water.

## Introduction

With the rapid promotion of urbanization, the radionuclides and precious metals pollution have become an imperative global environment problem, especially for europium (Eu) and Aurum (Au) (Zhao et al., 2015). Generally, europium has major applications in neutron protection, laser and atomic energy industry field, while gold is widely used in the fields of industry, agriculture and medicine (Neri et al., 2021, Zhao et al., 2021). However, a large amount of wastewater containing Eu(III) or Au(III) were produced in the process of application. Thereby, how to efficiently elimination of Eu(III) and Au(III) from the polluted water sources or industrial wastes to avoid these pollutants migration and transformation is a very pressing issue. In an effort to handle those challenges, several state-of-the-art techniques have been proposed to purify Eu(III) or Au(III)-containing wastewater, such as chemical precipitation (Yan et al., 2019), membrane processing (Wang et al., 2020), electrolysis (Liu et al., 2019) and adsorption (Zhang et al., 2019). Among them, adsorption seems to be one of the most effective and practical technologies owing to its simplicity and flexibility feature. Nowadays, different types of adsorbents have been developed and evaluated for Eu and Au ions clean-up, such as carbon nanotubes (Chen et al., 2008), graphene oxide (Ma et al., 2019), viscose fiber (Liu et al., 2020) and corn starch (Liu et al., 2019). However, these solid materials generally have the defects of low adsorption amounts, long equilibrium time and weak stability under various environmental conditions. One suggested approach is to the preparation of new materials with high adsorption capacity and high chemical stability, so that it can be used to efficient elimination of the two contaminant classes.

Recently, biomass materials have stimulated researchers' interest on account of their renewable, free of contamination and low cost characteristics (Zhu et al., 2021). So far, different types of bio-materials have been applied to eliminate the radionuclide and precious metals ions from the wastewater stream, such as tannin (Liu et al., 2021), chitosan (Liu et al., 2021) and cellulose (Zhang et al., 2021). Indeed,  $\beta$ -

cyclodextrin ( $\beta$ -CD) is also an inexpensive sustainable biomass resource, which is mainly produced from the enzymatic degradation of starch. More importantly,  $\beta$ -CD is cyclic oligosaccharides formed by 6–8 D-glucose units linked by  $\alpha$ -1,4-glucose bonds, which has been proved to exhibit good performance in wastewater disposal (Ghosh et al., 2011). However,  $\beta$ -CD requires a process of immobilization/insolubilization before being used as adsorbents for aqueous phase applications due to its water solubility. To compensate for this disadvantage, many efforts have been made to immobilize  $\beta$ -CD onto various water-insoluble matrices. For instance, Zhao et al. (Zhao et al., 2016) developed an EDTA- $\beta$ -cyclodextrin material to pre-concentration of Eu(III) from simulated seawater, and the maximum adsorption capacities reached up to 0.365 mmol/g. Martin-Trasanco et al. (Martin-Trasanco et al., 2017) reported a  $\beta$ -cyclodextrin polymer to selective recovery of Au(III) from acid medium, and it was observed that Au(III) ions could be efficient reduced to gold nano-particles by hydroxys groups. Guo et al. (Guo et al., 2015) synthesized a  $\text{Fe}_3\text{O}_4$ @cyclodextrin magnetic composite via a simple chemical co-precipitation method, and this magnetic composites could efficient removal of Eu(III) from industrial wastewater. Kyrychenko et al. (Slavgorodska et al., 2020) explored the adsorption behavior of  $\beta$ -cyclodextrin onto gold nano-particles, and it was found that  $\beta$ -CD binding onto the AuNP surface occurred through multiple non-covalent interactions. However, Although these surface modification strategies could effective immobilize  $\beta$ -CD on insoluble carrier, most of these methods use complicated procedures and toxic reagents, and the majority of the previously reported  $\beta$ -CD based adsorbents suffered from the low adsorption amounts and slow reaction rates toward the targeted contaminants. Consequently, there is an urgent need to propose a new  $\beta$ -CD immobilization strategy to elimination of the targeted pollutants. It is worth noting that waste paper (WP) is an inexpensive, renewable and massively available material, of which the main components are cellulose and hemicellulose. Notably, WP is easy to be oxidized by strong oxidant, which will produce a large amount of aldehyde groups on its skeleton. Furthermore, the aldehyde groups could form covalent and hydrogen bonds with the amine and hydroxy functional groups under the mild environmental conditions. Polyethylenimine a kind of sterically branched polymer with larger numbers of amino groups, such as primary, secondary and tertiary amine groups. And one third of the atoms of PEI are protonatable amino nitrogen atoms, which exhibits high affinity towards metal ions (Zhao et al., 2017). Hence, the special chemical structure of DAWP opened up an opportunity for the facile introduction of  $\beta$ -CD and PEI through one step or two-step synthetic strategies.

The purposes of this study were to: (1) to develop a novel bio-adsorbent (DAWP-PEI- $\beta$ -CD) via a facile two-step method and investigate its adsorption performance towards Eu(III) and Au(III) under various environmental conditions; (2) to characterize the as-synthesized bio-adsorbents by different physicochemical and spectroscopic techniques (FT-IR, XRD, SEM, NMR, XPS); (3) to evaluate the DAWP-PEI- $\beta$ -CD performance for Eu(III) and Au(III) uptake using the kinetic and isotherm models; (4) to understanding the interaction mechanism between DAWP-PEI- $\beta$ -CD and Eu(III)/Au(III) ions. This study will provide new clues to the overall recycling of Eu(III) and Au(III) in environmental pollution treatments.

## Materials And Methods

# Materials

$\beta$ -Cyclodextrin ( $\beta$ -CD, 98%), polyethyleneimine (PEI, M.W.600, 99%), epichlorohydrin (EPI, AR),  $\text{Eu}(\text{NO}_3)_3 \cdot 6\text{H}_2\text{O}$  (99.9%) and  $\text{HAuCl}_4 \cdot 4\text{H}_2\text{O}$  (99.9%) were purchased from Sinopharm Reagent Co. Ltd., China. The NaCl (99.5%),  $\text{FeCl}_2$  (98%),  $\text{NaIO}_4$  (99.5%), NaOH (95%), HCl (37%),  $\text{CuCl}_2$  (98%),  $\text{ZnCl}_2 \cdot 7\text{H}_2\text{O}$  (98%),  $\text{NiCl}_2 \cdot 6\text{H}_2\text{O}$  (99.9%),  $\text{FeCl}_3 \cdot 6\text{H}_2\text{O}$  (99%) and  $\text{K}_2\text{Cr}_2\text{O}_7$  (98%) were received by Shanghai Macklin Biochemical Co., Ltd. Waste paper (WP) was obtained from personal laboratory and crushed into small pieces mechanically before use.

## Preparation of DAWP-PEI- $\beta$ -CD

The preparation process of bio-adsorbent (DAWP-PEI- $\beta$ -CD) was proposed as Fig. 1. Firstly, 2 g of waste paper was firstly added into 60 mL of a sodium periodate solution (pH = 4.0, 0.7 mol/L). Then, the mixtures were stirred at 313 K for 5 h under exclusion of light, and the oxidized waste papers were obtained and named as DAWP. Secondly, 1 g of DAWP was added into 50 mL of PEI solution (5 wt.%) to form a suspension, which was continuous stirred at room temperature for 12 h to acquired yellow solids (DAWP-PEI). Finally, 4.8 g of EPI and 10 g of  $\beta$ -CD were dissolved into 100 mL of NaOH solution (7 wt.%). And then 2 g of DAWP-PEI was joined with the modification solution under intense stirring for 6 h. After that, the mixture was filtered with ultra-pure water to make it neutral and the as obtained bio-adsorbents (DAWP-PEI- $\beta$ -CD) were dried at in an oven for further use.

## Characterization

The Fourier transform infrared spectrometer (FT-IR) spectra were analyzed on the NEXUS 870 spectroscopy (Thermo, Madison, USA). X-ray photoelectron spectroscopy (XPS) data were registered in an ESCALAB 250 XPS (ThermoFisher, AlKa). The morphological analysis was carried out by scanning electron microscope (SEM) using a QUANTAFEG 400 (FEI company, USA), and elemental mapping was performed by Thermo Scientific Ultra Dry SDD Energy-dispersive X-ray spectroscopy (EDS, USA). The X-ray diffraction (XRD) analysis was performed on a Rigaku TTRIII diffractometer (Japan) with Cu K $\alpha$  irradiation over a  $2\theta$  range from 20 to 80°.  $^{13}\text{C}$  Solid state nuclear magnetic spectrum (NMR) were recorded on a Bruker AVANCE II 400WB spectrometer (Germany). Surface charge density of samples was determined by a Malvern Instruments Zetasizer Nano ZS90 (England).

## Batch removal experiments

Batch experiments were carried out to explore the capture performance of Eu(III) and Au(III) on DAWP-PEI- $\beta$ -CD. Here, 10 mg of DAWP-PEI- $\beta$ -CD was added into 50 mL of known concentration Eu(III) or Au(III) solution with the desired pH values. Then, the suspensions were shaken in the incubator at 250 rpm for 24 h until adsorption equilibrium. Upon the completion, the solid adsorbents were separated from solution phase by centrifugation. Subsequently, the supernatant concentration of Eu(III) was analyzed by the UV-vis adsorption spectrometer at the wavelengths 652 nm, whereas the residual concentration of Au(III) was conformed by ICP-AES. The adsorption ability of DAWP-PEI- $\beta$ -CD was performed by transferring 10 mg of bio-adsorbents into 50 mL of targeted pollutants, which already contained a series

of different concentrations of Eu(III) and Au(III) solution. The kinetic experiment of Au(III) and Eu(III) on DAWP-PEI- $\beta$ -CD were carried out at optimal pH values, and the concentrations of metal ions were measured and recorded at different time points until adsorption equilibrium. The adsorbed amounts of Eu(III) and Au(III) onto DAWP-PEI- $\beta$ -CD were calculated from the difference of initial concentration and final concentration remained in solution after equilibrium.

## Results And Discussion

### Adsorbent characterization

XPS analyses were used to investigate the surface chemical compositions of DAWP, DAWP-PEI and DAWP-PEI- $\beta$ -CD. As showed in Fig. 2, the C1s spectrum of DAWP could be quantitatively resolved into three bonds at 284.81, 286.62 and 288.12 eV corresponded to carbon-carbon bond (C-C), carbon-oxygen bond (C-OH) and carbon and oxygen double bond (C = O), respectively. Interestingly, once the PEI molecules were immobilized on DAWP via Schiff base reaction, two new peaks appeared at 287.15 eV (C = N) and 285.74 eV (C-N), proving that a mass of amino groups existed on the surface of DAWP-PEI (Liu et al., 2020). However, as the  $\beta$ -CD molecules were further introduced into DAWP-PEI through cross-linking reaction, the relative content of C-N on DAWP-PEI (14.20%) was lower than that of DAWP-PEI- $\beta$ -CD (25.58%), and other characteristic peaks were still presented in DAWP-PEI- $\beta$ -CD. These observations conformed that PEI and  $\beta$ -CD molecules had been successfully immobilized on DAWP via a facile two-step method.

FT-IR measurements were mostly used in order to confirm the formation of functional groups. Thus, different functional groups were detected in the IR spectra of  $\beta$ -CD, DAWP, DAWP-PEI and DAWP-PEI- $\beta$ -CD. In Fig. 2d, the typical peaks of  $\beta$ -CD at  $3352\text{ cm}^{-1}$  and  $1208\text{ cm}^{-1}$  were generated by the -OH and -CH<sub>2</sub> bending vibrations, whereas another band at  $1059\text{ cm}^{-1}$  was produced by inverse-symmetric glycosidic (Wang et al., 2014). The bands centered at  $1688\text{ cm}^{-1}$ ,  $1427\text{ cm}^{-1}$  and  $1109\text{ cm}^{-1}$  ascribed to -C = O, -CH<sub>2</sub> and C-O-C stretching vibrations of DAWP, respectively (Liu et al., 2019). Notably, once the PEI molecules were introduced into oxidized waste paper, two regular peaks appeared at  $1649\text{ cm}^{-1}$  and  $1422\text{ cm}^{-1}$  corresponded to -C = N and -NH<sub>2</sub>, respectively (Al-Harashsheha et al., 2020). Interestingly, after the cross-linking reaction, the characteristic peaks of  $\beta$ -CD and PEI were also appeared at the IR spectra of DAWP-PEI- $\beta$ -CD, such as primary amine ( $1455\text{ cm}^{-1}$ ) and the b(1-4) skeleton vibrations ( $1033\text{ cm}^{-1}$ ). These analysis results further proved that the  $\beta$ -CD and PEI were successfully introduced into the oxidized waste paper.

The chemical structure of all adsorbents was further assessed by solid state NMR measurements. In Fig. 3, one can see that the broad signals from 102 ppm to 59 ppm were attributed to the carbon atoms in  $\beta$ -CD, and the signals at  $\delta = 63, 72, 84$  and  $102$  ppm corresponding to C-d, C-a, C-e and C-b, respectively (Shen et al., 2015). Compared with  $\beta$ -CD, the characteristic peak of carbon atoms at  $\delta = 72$  ppm (C-2) and  $65$  ppm (C-4) were almost overlapped or disappeared in the NMR spectrum of DAWP, which may be

related to the signal amplification of C-5 and C-3 after oxidation reaction. However, when DAWP was reacted with PEI, there were several new characteristic peaks appeared at NMR spectra of DAWP-PEI. For instance, the carbon and nitrogen double bond (C = N) as well as carbon and nitrogen single bond (C-N) were observed at  $\delta = 143$  ppm and 30 ppm, respectively. Interestingly, most of DAWP and PEI's carbon atom signals were also detected on the NMR spectra of DAWP-PEI- $\beta$ -CD after cross-linking reaction, and a different signal appeared at  $\delta 169$  ppm may ascribed to C = O. These results were in accordance with FT-IR and XPS results, which further manifested that the successful cross-linking between DAWP and  $\beta$ -CD/PEI.

## Influences of pH values

As is well-known, solution pH not only can affect the relative distribution of pollutants species but also change the surface charge of adsorbents. Thus, the adsorption abilities of DAWP-PEI- $\beta$ -CD towards Eu(III) and Au(III) were investigated in this work. As depicted in Fig. 3a, adsorption amounts of Eu(III) on DAWP-PEI- $\beta$ -CD were up to 282 mg/g rapidly from 2.0 to 5.0, subsequently maintained the high level within pH the range of 6.0–9.0, which implied that solution pH played a vital role in elimination of contaminants. This phenomenon could be explained by the relative distribution of Eu(III) species and the surface charge of DAWP-PEI- $\beta$ -CD. It was reported that Eu(III) ions were mainly presented as  $\text{Eu}^{3+}$  species at pH < 5.0 in water solution, and then  $\text{Eu}(\text{OH})^{2+}$  and  $\text{Eu}_2(\text{OH})_2^{4+}$  species began to increase with pH further increasing (Li et al., 2020). Meanwhile, zeta potential analyzer determined the surface charge density of DAWP-PEI- $\beta$ -CD was 3.29 (Fig. S1). Thus, according to Coulomb's law, the positive charge of Eu(III) species were more easily adsorbed on the negatively charged DAWP-PEI- $\beta$ -CD through electrostatic attraction. However, the adsorption behavior of Au(III) was significantly different from that of Eu(III) at various pH values. In Fig. 3b, one can see that adsorbed amounts of Au(III) on DAWP-PEI- $\beta$ -CD increased sharply as pH values were raised from 1.0 to 2.0, and then sharply decreased over the pH range 2.0–6.0, and achieving its best performance at pH 2.0. Such a pH-dependent adsorption can be explained from the point of view of the following aspects. At lower pH values, the Au(III) ions were mainly existed as  $\text{AuCl}_4^-$ , which were favorable to capture on the positively-charged DAWP-PEI- $\beta$ -CD via electrostatic interactions. Notably, the chloride ion occupied a part of the active sites during adsorption process at pH < 2.0, which led to a lower adsorption amounts (Wang et al., 2015). However, under high pH conditions, the negative charge increased on the surface of DAWP-PEI- $\beta$ -CD and the electrostatic repulsion would occur between the bio-adsorbents and adsorbates at high pH values.

## Adsorption isotherms and thermodynamic studies

The adsorption isotherms are an important factor in understanding the adsorption efficiency and studying the adsorption mechanism. Figure 5 displays the relationship between the residual Eu(III) and Au(III) concentrations and the equilibrium adsorption capacities on DAWP-PEI- $\beta$ -CD at room temperature. Evidently, along with the initial concentration increasing, the adsorption amounts of Eu(III) and Au(III) on DAWP-PEI- $\beta$ -CD rapidly increased at the beginning and then tended to adsorption equilibrium. Interestingly, the equilibrium adsorption capacities of Au(III) were both higher than that of Eu(III) on DAWP-PEI and DAWP-PEI- $\beta$ -CD, which was evident that the greater affinity to Au(III) than Eu(III) in the

adsorption process. To determine the saturated capture amounts and sorption type, the Langmuir and Freundlich equations were applied to fit the experimental data, and the detailed fitting results were provided in Fig. 5 and Table S1. As expected, the results of calculation and simulation showed that the adsorption behavior of Eu(III) and Au(III) were fitted well by the Langmuir model, which indicated that uptake of the two targeted contaminants onto DAWP-PEI- $\beta$ -CD surfaces was localized in a monolayer (Yang et al., 2019). Besides, the adsorption thermodynamics of Eu(III) and Au(III) on DAWP-PEI- $\beta$ -CD were also measured using the Gibbs equations. As listed in Table S2, the spontaneous and endothermic adsorption processes were revealed by the negative  $\Delta G^\circ$  and positive  $\Delta H^\circ$  values, whereas the negative  $\Delta S^\circ$  reflected a decrease in the randomness during the adsorption process. Notably, the maximum uptake amounts of DAWP-PEI- $\beta$ -CD for single Eu(III) and Au(III) were 241.3 and 424.2 mg mg/g, which were far higher than that of the reported available materials (Table S3). Such a high adsorption amount could be ascribed to the special chemical structure and the large cavities, which were advantageous for accommodating more Eu(III) and Au(III).

## Adsorption kinetics

Adsorption kinetics not only focuses on the relationship between adsorption capacity and adsorption time, but also evaluate the rate of the interaction process. Figure 6 illustrates the time-dependent experiments of Eu(III) and Au(III) adsorbed onto DAWP-PEI- $\beta$ -CD. As expected, the concentration of targeted contaminants rapidly declined during the initial phase, and then tend to a constant value with the extension of incubation time. The rapid adsorption in the beginning may be due to the greater concentration gradient and more available sites for adsorption. Subsequently, the active sites were gradually depleted, resulting in the final adsorption equilibrium. Note that the Au(III) exhibited faster kinetics compared with Eu(III) at optimal water environmental condition, which suggested that Eu(III) ions took a relatively longer time to diffuse into the interlayer of DAWP-PEI- $\beta$ -CD. To figure out the adsorption rate and rate determining step, different kinetic models were applied to simulate the kinetic data, and the corresponding fitting curves and parameters were displayed in Fig. 6 and Table S4. According to the fitted results, on can see that the PFO equation either overestimated or underestimated the kinetics behavior of Eu(III) and Au(III) on DAWP-PEI- $\beta$ -CD, while the PSO model could well simulate the kinetic process from the beginning to the end, and the calculated limits of quantification were close to the experimental limits of quantification, which implied that uptake of the two targeted pollutants mainly depended on chemical adsorption (Cheng et al., 2018, Wang et al., 2019). To further identify the main rate-controlling step, the kinetic data were further analyzed by the Intraparticle diffusion equation, and the plots of  $qt$  vs.  $t^{1/2}$  were displayed in Fig. 6c, d. The simulation results exhibited that the lines do not pass through the origin and tend to be multilinear, which manifested that the rate controlling steps did not only include intraparticle diffusion, and other reactions according to the definition of the equation (Qiu et al., 2020, Hu et al., 2021).

## Selectivity test

Considering the practical application of the targeted pollutants removal from industrial wastewater, the effect of competing ions of adsorbents were also important. Thus, the selective binding ability of DAWP-PEI- $\beta$ -CD towards Eu(III) and Au(III) was investigated in a mixed system, in which the concentration of

metal ions were all controlled at 50 mg/L. In Fig. S2, one can see that the adsorption capacity of Au(III) on DAWP-PEI- $\beta$ -CD was calculated as 209 mg/g in single system, and that was reduced by 20.1% in mixed system. This phenomenon occurred due to most of co-existing metal ions existed as their cationic or neutral forms, while Au(III) ions were mainly existed as  $\text{AuCl}_4^-$  in acidic solution. Thus, the negatively charged Au(III) species could occupy more adsorption sites on the surface of DAWP-PEI- $\beta$ -CD, which led to a high Au(III) adsorption amounts. Besides, it should be pointed out that the molecular structure of Eu(III) were similar to that of Au(III) to some extent, but the removal amounts of Eu(III) was still lower than that of Au(III) at this adsorption conditions. This may be due to the electrostatic repulsion occurred between Eu(III) ions during adsorption process. This result manifested that DAWP-PEI- $\beta$ -CD exhibited high selectivity for Au(III) against other co-existing pollutants in the multi-solute system.

## Elimination mechanisms

To find out the detailed elimination mechanism, the as-prepared bio-adsorbent's surface properties and specific elemental constituents were explored by SEM, XPS and XRD after binding with Eu(III) and Au(III). In Fig. 7, one can see that the main components of DAWP-PEI- $\beta$ -CD were C, H, N and O, whereas the element Eu and Au were spread over the whole surface of DAWP-PEI- $\beta$ -CD-Eu and DAWP-PEI- $\beta$ -CD-Au, suggesting that DAWP-PEI- $\beta$ -CD could efficient enrichment of Eu(III) and Au(III) from water environment. Interestingly, in Fig. 8a, in addition to C1s and O1s, the spent DAWP-PEI- $\beta$ -CD's surface also appeared characteristic peaks of Eu3d and Au4f, which was consistent with the results analyzed in EDS, further proved that the successful immobilization of the two targeted pollutants onto DAWP-PEI- $\beta$ -CD.

To resolve the chemical properties and states of Eu and Au atoms on the DAWP-PEI- $\beta$ -CD, the high-resolution spectra of Eu3d and Au4f were further resolved by deconvolution method. In Fig. 8b, one could see that two main peaks located at 1134.49 eV ( $\text{Eu}3d_{3/2}$ ) and 1164.16 eV ( $\text{Eu}3d_{5/2}$ ) in the high-resolution Eu3d spectrum corresponded to the Eu(III) signals, which implied that only Eu(III) ions existed on the surface of DAWP-PEI- $\beta$ -CD, and the surface complexes reaction dominated the processes of Eu(III) uptake on DAWP-PEI- $\beta$ -CD (Huang et al., 2018). However, In Fig. 8c, the Au4f peak was mainly consisted of  $\text{Au}4f_{7/2}$  and  $\text{Au}4f_{5/2}$ , each of which could be further divided into Au(III) and Au(0). Specifically, the peaks at 83.36 eV ( $\text{Au}4f_{7/2}$ ) and 87.08 eV ( $\text{Au}4f_{5/2}$ ) corresponded to Au(III), whereas the signatures at 84.18 eV ( $\text{Au}4f_{7/2}$ ) and 89.05 eV ( $\text{Au}4f_{5/2}$ ) were ascribed to Au(0), which demonstrated that a large amount of Au(0) existed onto the surface of spent bio-adsorbents (Pestov et al., 2015). This result was further proved by the XRD analysis. In Fig. 8e, one can see that the powder XRD patterns of DAWP-PEI- $\beta$ -CD exhibited two major peaks at  $2\theta = 12.3^\circ$  and  $18.1^\circ$ , which may be ascribed to the characteristic peak of  $\beta$ -CD. However, after adsorption of Au(III), there were four the high intensity peaks appeared at the XRD patterns of DAWP-PEI- $\beta$ -CD-Au, and the reflections of elemental gold were observed at  $2\theta = 38.19^\circ$ ,  $44.38^\circ$ ,  $64.71^\circ$  and  $77.52^\circ$  with the corresponding planes of (111), (200), (220) and (311). Noticeably, the specific area percentage of C = O enhanced from 12.09 % to 15.78%, and the content of Au(0) reached up to 54.65% after adsorption of Au(III) (see Table S5). These phenomena illustrated that part of surface adsorbed Au(III) has been reduced to Au(0) during the Au(III) capture processes. Besides, in Fig. 8f, the N1s peaks shifted from 398.86 eV to 399.09 eV after Au(III) adsorption, while it was shifted from 398.86

eV to 399.52 eV after Eu(III) adsorption, which illuminated that the nitrogen containing functional groups played roles not only as a cross-linker but also as adsorption sites for Eu(III) and Au(III). On the basis of characterization analysis as well as adsorption experiments, the mechanism of removing the targeted contaminant by DAWP-PEI- $\beta$ -CD was schematically illustrated in Fig. 9. The mechanism of Eu(III) removal by DAWP-PEI- $\beta$ -CD was mainly through the surface coordination and host-guest inclusion interaction. Specifically, on the one hand, the ample amino groups of DAWP-PEI- $\beta$ -CD that could form complex compounds with Eu(III). On the other hand, the cavities of  $\beta$ -CD could make contributions to the host-guest inclusion complexes with Eu(III). However, the adsorption mechanism of Au(III) on DAWP-PEI- $\beta$ -CD was mainly attributed to the electrostatic attraction, chelation, host-guest inclusion, and redox reaction. Once the fresh DAWP-PEI- $\beta$ -CD was exposed to Au(III) solution, the targeted contaminants were rapidly enriched onto DAWP-PEI- $\beta$ -CD surface via electrostatic interaction and followed the reduction of a part of Au(III) to Au(0) with the help of reductive functional groups. Finally, most of Au(III) and Au(0) were immobilized on the surface of DAWP-PEI- $\beta$ -CD by the host-guest inclusion interaction.

## Conclusion

In summary, a novel bio-adsorbent (DAWP-PEI- $\beta$ -CD) was synthesized by grafting PEI and  $\beta$ -CD into dialdehyde waste paper via a facile two-step method. Characterization results found that the  $\beta$ -CD and amino groups played an important role in uptake of Eu(III) and Au(III). Batch experiment showed that the isotherm and kinetic data were fitted well to the Langmuir and Pseudo-second-order models, and the saturated adsorption capacity of Eu(III) (pH = 6.0) and Au(III) (pH = 2.0) onto DAWP-PEI- $\beta$ -CD were 424.2 and 241.3 mg/g, respectively. The thermodynamic parameters suggested that the adsorption of Eu(III) and Au(III) on DAWP-PEI- $\beta$ -CD were a spontaneous and endothermic processes. The adsorption mechanism study revealed that the elimination of Eu(III) was attributed to host-guest inclusion and surface complexation interactions, whereas adsorption of Au(III) might stem from a combination of electrostatic attraction, chelation, host-guest inclusion and oxidation-reduction interaction. Thus, these results will facilitate the development of new type biomass-based materials for Eu(III) and Au(III) pollution cleanup.

## Declarations

## Acknowledgment

We gratefully thank the Research Fund Program of National Natural Science Foundation of China (No. 21876115), Zhejiang Public Welfare Technology Application and Social Development Project (LGF21C030001).

## Author contributions

Fenglei Liu, Shan Hua: Investigation, Data curation, Writing-original draft. Qingyuan Hu: Investigation, Project administration. Baowei Hu: Writing-review & editing.

## Availability of data and material

All data are available from the authors upon reasonable request.

## Conflict of interest

There are no conflicts of interest do declare.

## References

1. Al-Harashsheha M, AlJaraha M, Alrebakia M, Mayyasb M (2020) Nanoionic exchanger with unprecedented loading capacity of uranium. *Sep Purif Technol* 238:116423
2. Chen C, Hu J, Xu D, Tan X, Meng Y, Wang X (2008) Surface complexation modeling of Sr(II) and Eu(III) adsorption onto oxidized multiwall carbon nanotubes. *J Colloid Interf Sci* 323: 33–41
3. Chen X, Yang X, Xiang Y, Xu L, Liu G (2020) Humic acid derived resin: an efficient adsorbent for Au(III) uptake from aqueous acidic solution. *J Chem Eng Data* 65: 1824–1832
4. Cheng W, Wan T, Wang X, Wu W, Hu B (2018) Plasma-grafted polyamine/hydrotalcite as high efficient adsorbents for retention of uranium (VI) from aqueous solutions. *Chem Eng J* 324: 103–111.
5. Fang Q, Duan S, Zhang J, Li J, Leung K (2017) Dual shelled  $Fe_3O_4$ /polydopamine hollow microspheres as an effective Eu(III) adsorbent. *J Mater Chem A* 5: 2947–2958
6. Ghosh S, Badruddoza AZM, Uddin MS, Hidajat K (2011) Adsorption of chiral aromatic amino acids onto carboxymethyl- $\beta$ -cyclodextrin bonded  $Fe_3O_4/SiO_2$  core-shell nanoparticles. *J Colloid Interf Sci* 354: 483–492
7. Guo Z, Li Y, Pan S, Xu J (2015) Fabrication of  $Fe_3O_4$ @cyclodextrin magnetic composite for the high-efficient removal of Eu(III). *J Mol Liq* 206: 272–277
8. Hu B, Wang H, Liu R, Qiu M (2021) Highly efficient U(VI) capture by amidoxime/carbon nitride composites: Evidence of EXAFS and modeling. *Chemosphere*. 274: 129743.
9. Huang S, Pang H, Li L, Jiang S, Wen T, Zhuang L, Hu B, Wang X (2018) Unexpected ultrafast and high adsorption of U(VI) and Eu(III) from solution using porous  $Al_2O_3$  microspheres derived from MIL-53. *Chem Eng J* 353: 157–166.
10. Liu H, Zhou Y, Yang Y, Zou K, Wu R, Xia K, Xie S (2019) Synthesis of polyethylenimine/graphene oxide for the adsorption of U(VI) from aqueous solution. *Appl Surf Sci* 471: 88–95
11. Liu F, Wang S, Chen S (2020) Adsorption behavior of Au(III) and Pd(II) on persimmon tannin functionalized viscose fiber and the mechanism. *Int J Biol Macromol* 152: 1242–1251

12. Liu F, Peng G, Li T, Yu G, Deng S (2019) Au(III) adsorption and reduction to gold particles on cost-effective tannin acid immobilized dialdehyde corn starch. *Chem Eng J* 370: 228–228 23
13. Liu F, Zhou Z, Li G (2021) Persimmon tannin functionalized polyacrylonitrile fiber for highly efficient and selective recovery of Au(III) from aqueous solution. *Chemosphere* 264: 128469
14. Liu F, Hua S, Zhou L, Hu B (2021) Development and characterization of chitosan functionalized dialdehyde viscose fiber for adsorption of Au(III) and Pd(II). *Int J Biol Macromol* 173: 457–466
15. Liu F, Zhou L, Wang W, Yu G, Deng S (2020) Adsorptive recovery of Au(III) from aqueous solution using crosslinked polyethyleneimine resins. *Chemosphere* 241: 125122
16. Liu F, Peng G, Li T, Yu G, Deng S (2019) Au(III) adsorption and reduction to gold particles on cost-effective tannin acid immobilized dialdehyde corn starch. *Chem Eng J* 370: 228–236
17. Li S, Dong L, Wei Z, Sheng G, Hu B (2020) Adsorption and mechanistic study of the invasive plant-derived biochar functionalized with CaAl-LDH for Eu(III) in water. *J Environ Sci* 96: 127–137.
18. Ma J, Zhao Q, Zhou L, Wen T, Wang J (2019) Mutual effects of U(VI) and Eu(III) immobilization on interpenetrating 3-dimensional MnO<sub>2</sub>/graphene oxide composites. *Sci Total Environ* 695: 133696
19. Martin-Trasanco R, Cao R, Esparza-Ponce HE, Montero-Cabrera ME (2017) Reduction of Au(III) by a  $\beta$ -cyclodextrin polymer in acid medium, a stated unattainable reaction. *Carbohydr Polym* 175: 530–537
20. Neri G, Cordaro A, Cordaro SM, Mazzaglia A, Piperno A (2021) PEGylated bis-adamantane carboxamide as guest bridge for graphene poly-cyclodextrin gold nanoassemblies. *J Mol Struct* 1240: 130519
21. Qiu M, Liu Z, Wang S, Hu B (2020) The photocatalytic reduction of U(VI) into U(IV) by ZIF-8/g-C<sub>3</sub>N<sub>4</sub> composites at visible light. *Environ Res* 11: 110349.
22. Pestov A, Nazirov A, Modin E, Mironenko A, Bratskaya S (2015) Mechanism of Au(III) reduction by chitosan: Comprehensive study with <sup>13</sup>C and <sup>1</sup>H NMR analysis of chitosan degradation products. *Carbohydr Polym* 117: 70–77
23. Slavgorodska MV, Kyrychenko A (2020) Adsorption behavior of  $\beta$ -cyclodextrin onto gold nanoparticles. *J Mol Graph Model* 94: 107483
24. Shen H, Zhu G, Yu W, Wu H, Ji H, Shi H, She Y, Zheng Y (2015) Fast adsorption of p-nitrophenol from aqueous solution using  $\beta$ -cyclodextrin grafted silica gel. *Appl Surf Sci* 356: 1155–1167
25. Sun Y, Chen C, Tan X, Shao D, Li J, Zhao G, Yang S, Wang Q, Wang X (2012) Enhanced adsorption of Eu(III) on mesoporous Al<sub>2</sub>O<sub>3</sub>/expanded graphite composites investigated by macroscopic and microscopic techniques. *Dalton Trans* 41: 13388–13394
26. Wang J, Wang Y, Wang W, Pen T, Liang J, Li P, Pan D, Fan Q, Wu W (2020) Visible light driven Ti<sup>3+</sup> self-doped TiO<sub>2</sub> for adsorption-photocatalysis of aqueous U(VI). *Environmen Pollut* 262: 114373
27. Wang H, Liu Y, Zeng G, Hu X, Hu X, Li T, Li H, Wang Y, Jiang L (2014) Grafting of  $\beta$ -cyclodextrin to magnetic graphene oxide via ethylenediamine and application for Cr(VI) removal. *Carbohydr Polym* 113: 166–173

28. Wang F, Zhao J, Zhu M, Yu J, Hu Y, Liu H (2015) Selective adsorption-deposition of gold nanoparticles onto monodispersed hydrothermal carbon spherules: a reduction-deposition coupled mechanism. *J Mater Chem A* 3: 1666–1674.
29. Wang M, Cheng W, Wan T, Hu BW, Zhu YL, Song XF, Sun YB (2019) Mechanistic investigation of U(VI) sequestration by zero-valent iron/activated carbon composites. *Chem Eng J* 362: 99–106.
30. Yan Z, Huang Q, Wang L, Zhang F (2019) Synthesis of tailored bis-succinamides and comparison of their extractability for U(VI), Th(IV) and Eu(III). *Sep Purif Technol* 213: 322–327
31. Yang S, Li Q, Chen L, Chen Z, Pu Z, Wang H, Yu S, Hu B, Chen J, Wang X (2019) Ultrahigh sorption and reduction of Cr(VI) by two novel core-shell composites combined with Fe<sub>3</sub>O<sub>4</sub> and MoS<sub>2</sub>. *J Hazard Mater* 379: 120797.
32. Zhao F, Repo E, Yin D, Meng Y, Jafari S, Sillanpää M (2015) EDTA-cross-linked βcyclodextrin: an environmentally friendly bifunctional adsorbent for simultaneous adsorption of metals and cationic dyes. *Environ Sci Technol* 49: 10570–10580
33. Zhao B, Yuan L, Wang Y, Duan T, Shi W (2021) Carboxylated UiO-66 tailored for U(VI) and Eu(III) trapping: from batch adsorption to dynamic column separation. *ACS Appl Mater Interfaces* 13: 16300–16308
34. Zhang Q, Zhao D, Feng S, Wang Y, Jin J, Alsaedi A, Hayat T, Chen C (2019) Synthesis of nanoscale zero-valent iron loaded chitosan for synergistically enhanced removal of U(VI) based on adsorption and reduction. *J Colloid Interf Sci* 552: 735–743
35. Zhu Y, Wang X, Li Z, Fan Y, Zhang X, Chen J, Zhang Y, Dong C, Zhu Y (2021) Husbandry waste derived coralline-like composite biomass material for efficient heavy metal ions removal. *Bioresour Technol* 337: 125408
36. Zhang M, Dong Z, Hao F, Xie K, Qi W, Zhai M, Zhao L (2021) Ultrahigh and selective adsorption of Au(III) by rich sulfur and nitrogen-bearing cellulose microspheres and their applications in gold recovery from gold slag leaching solution. *Sep Purif Technol* 274: 119016
37. Zhao F, Repo E, Meng Y, Wang X, Yin D, Sillanpää M (2016) An EDTA-β-cyclodextrin material for the adsorption of rare earth elements and its application in preconcentration of rare earth elements in seawater. *J Colloid Interf Sci* 465: 215–224
38. Zhao F, Repo E, Song Y, Yin D, Hammouda SB, Chen L, Kalliola S, Tang J, Tam KC, Sillanpää M (2017) Polyethylenimine-cross-linked cellulose nanocrystals for highly efficient recovery of rare earth elements from water and a mechanism study. *Green Chem* 19: 4816–4828

## Figures

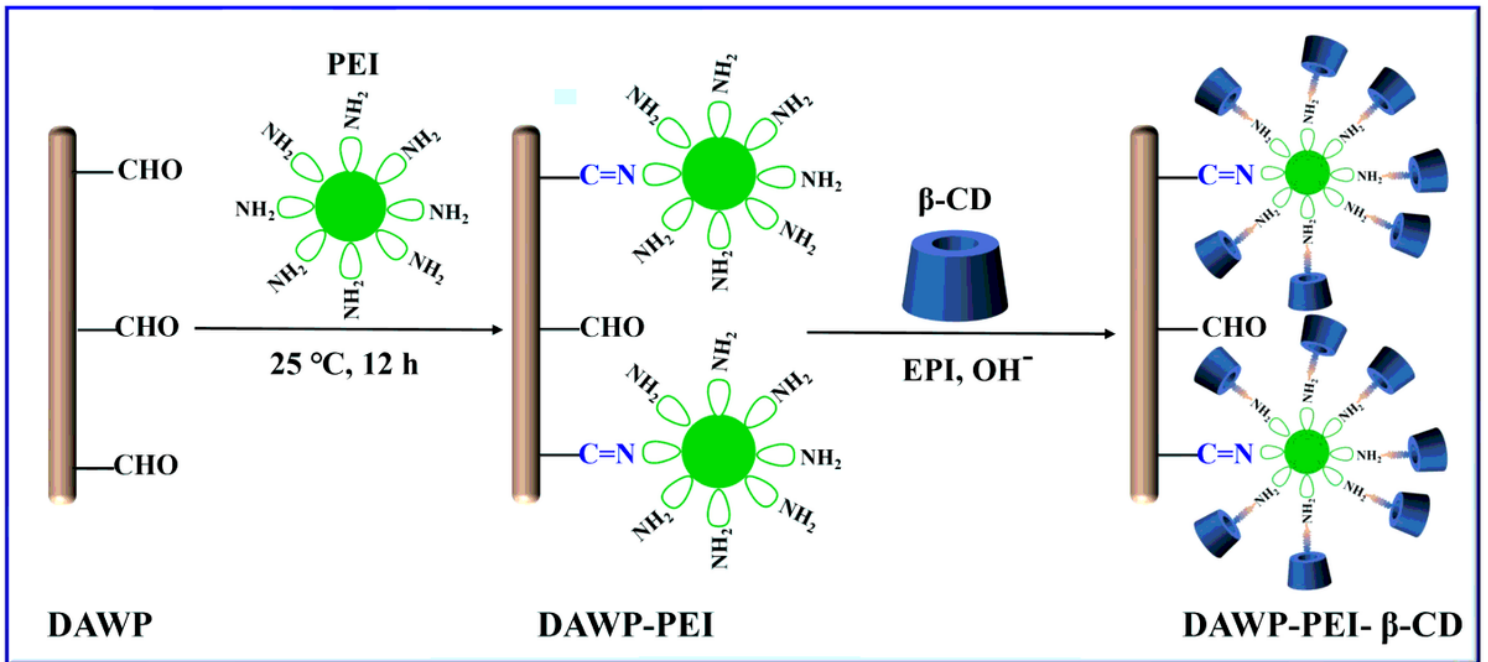
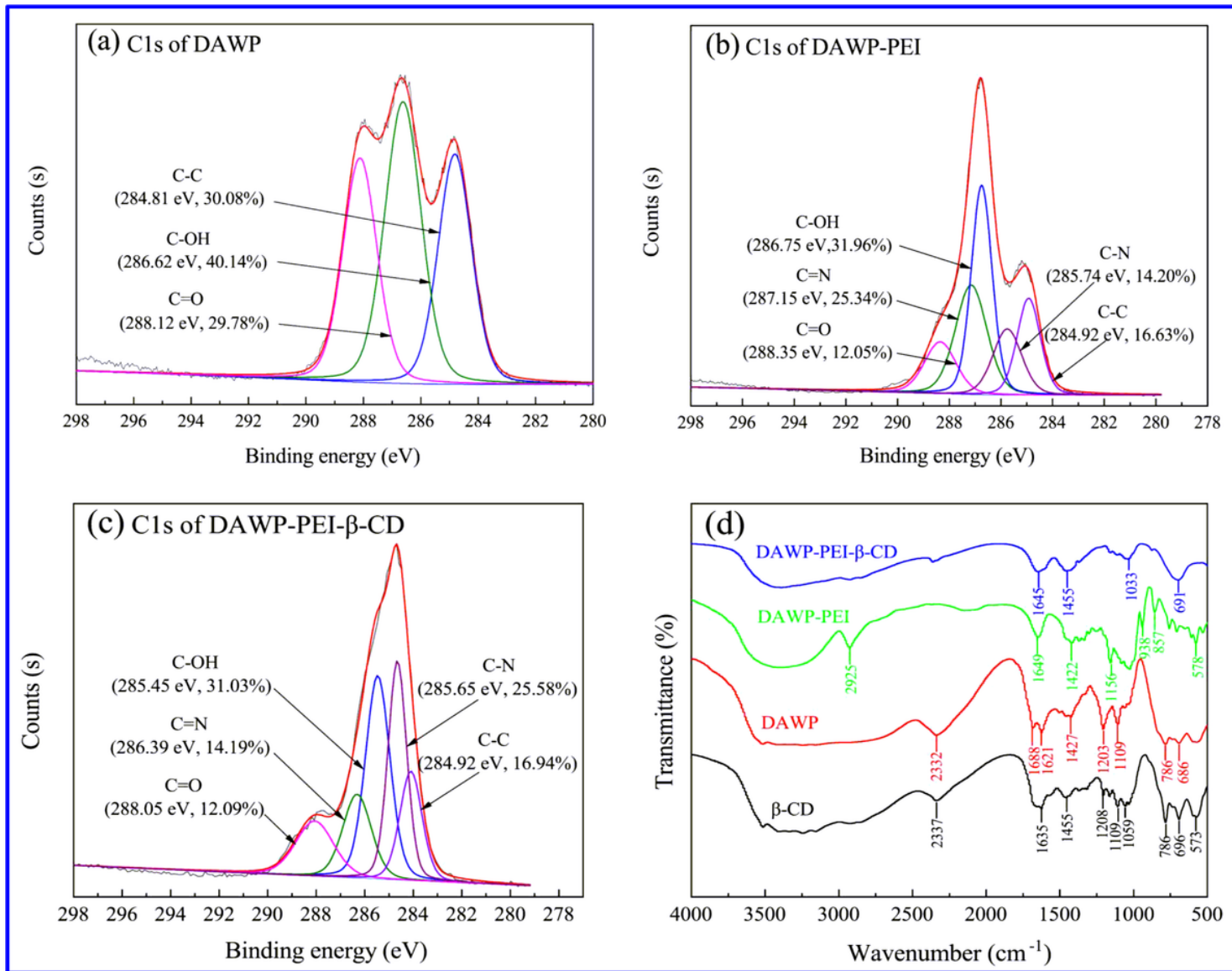


Figure 1

Schematic diagrams for the synthetic procedures of DAWP-PEI-β-CD.



**Figure 2**

XPS C1s spectrum (a, b, c) and FT-IR (d) of β-CD, DAWP, DAWP-PEI and DAWP-PEI-β-CD.

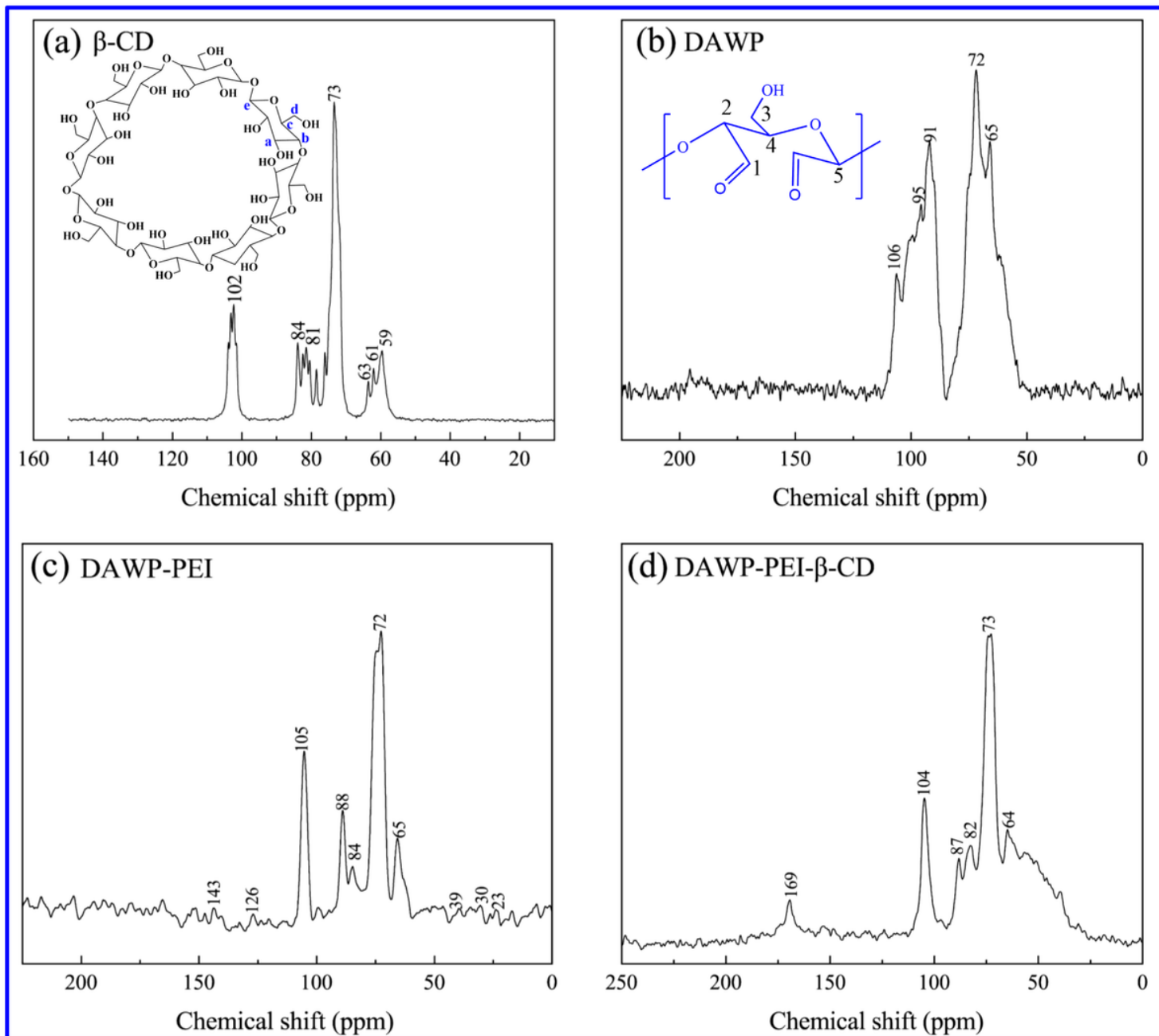


**Figure 3**

$^{13}\text{C}$  NMR spectra of  $\beta\text{-CD}$ , DAWP, DAWP-PEI and DAWP-PEI- $\beta\text{-CD}$ .

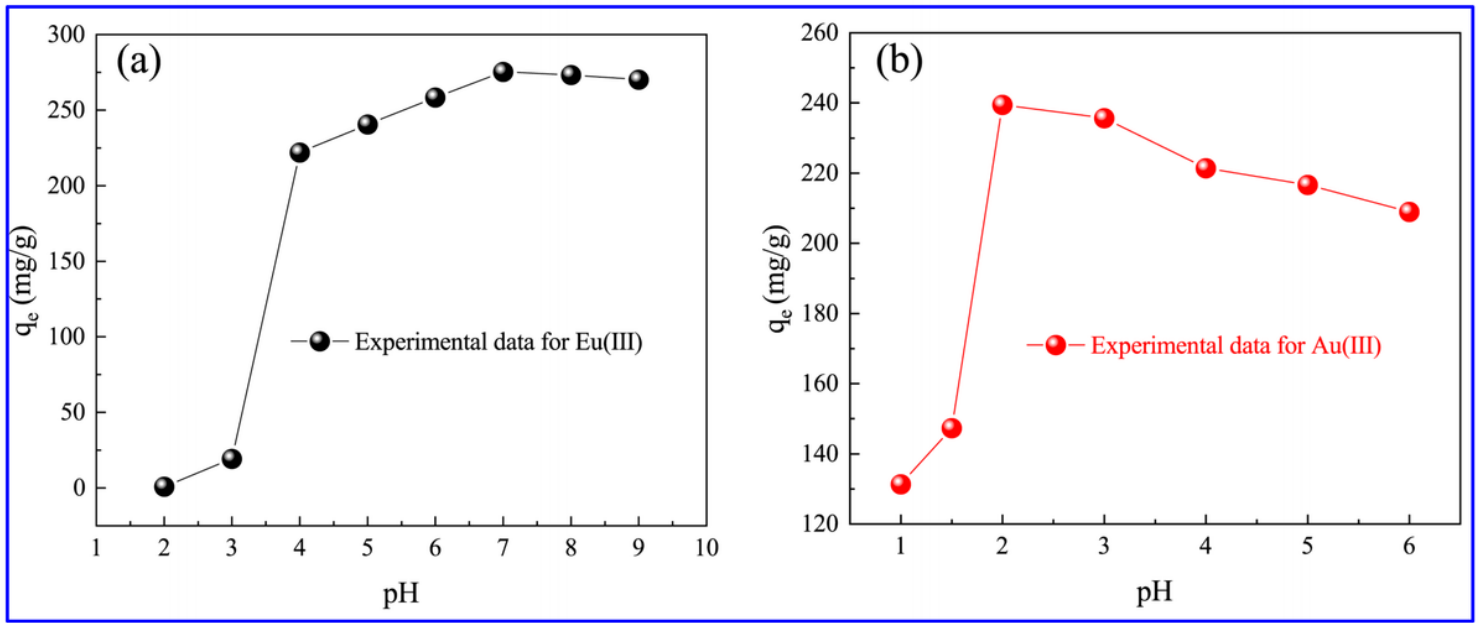


**Figure 4**

Effect of initial pH on elimination of Eu(III) and Au(III) by DAWP-PEI- $\beta$ -CD.

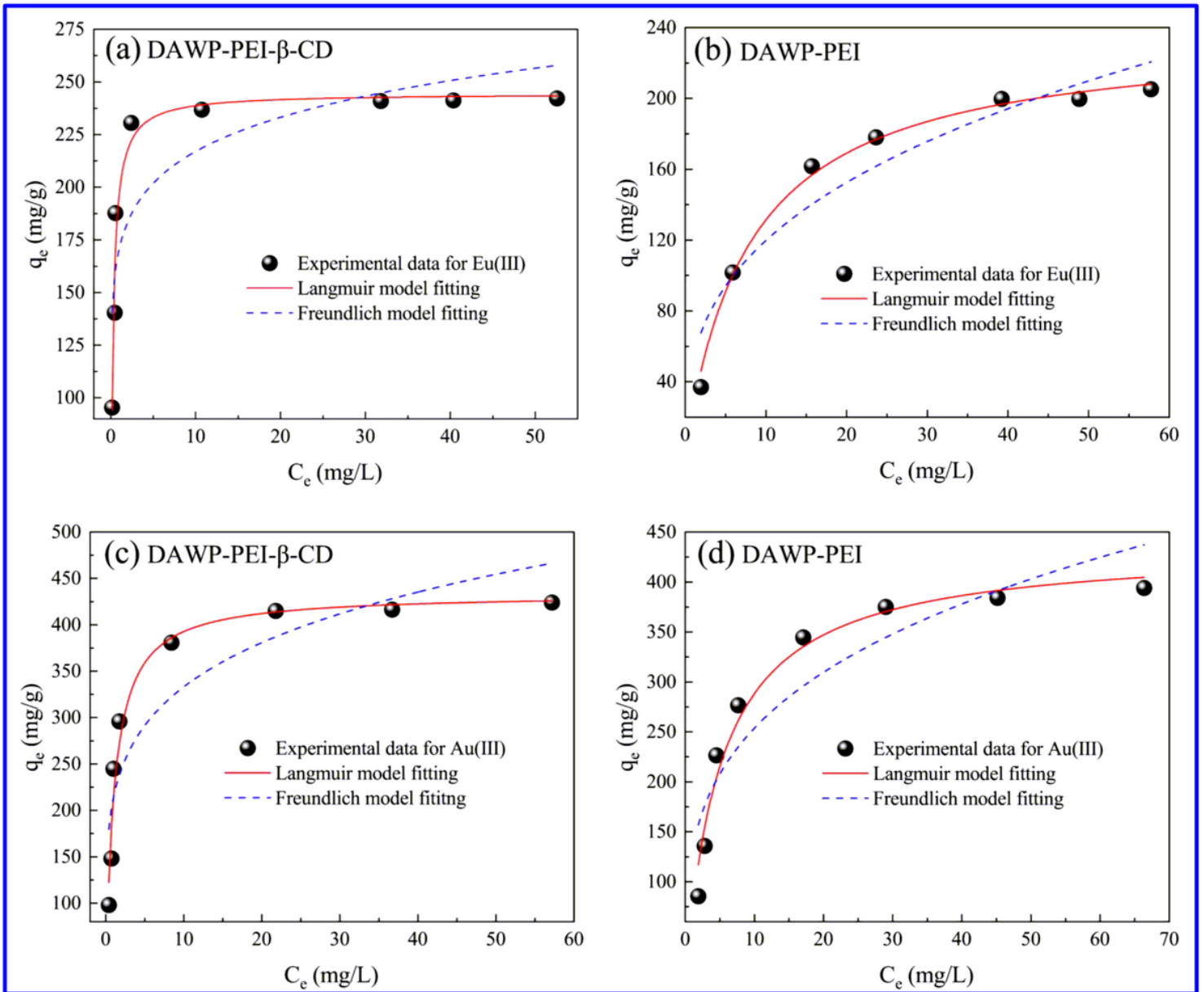


**Figure 5**

Sorption isotherms of Eu(III) and Au(III) on DAWP-PEI and DAWP-PEI- $\beta$ -CD as well as fitting by the Langmuir and Freundlich equations.

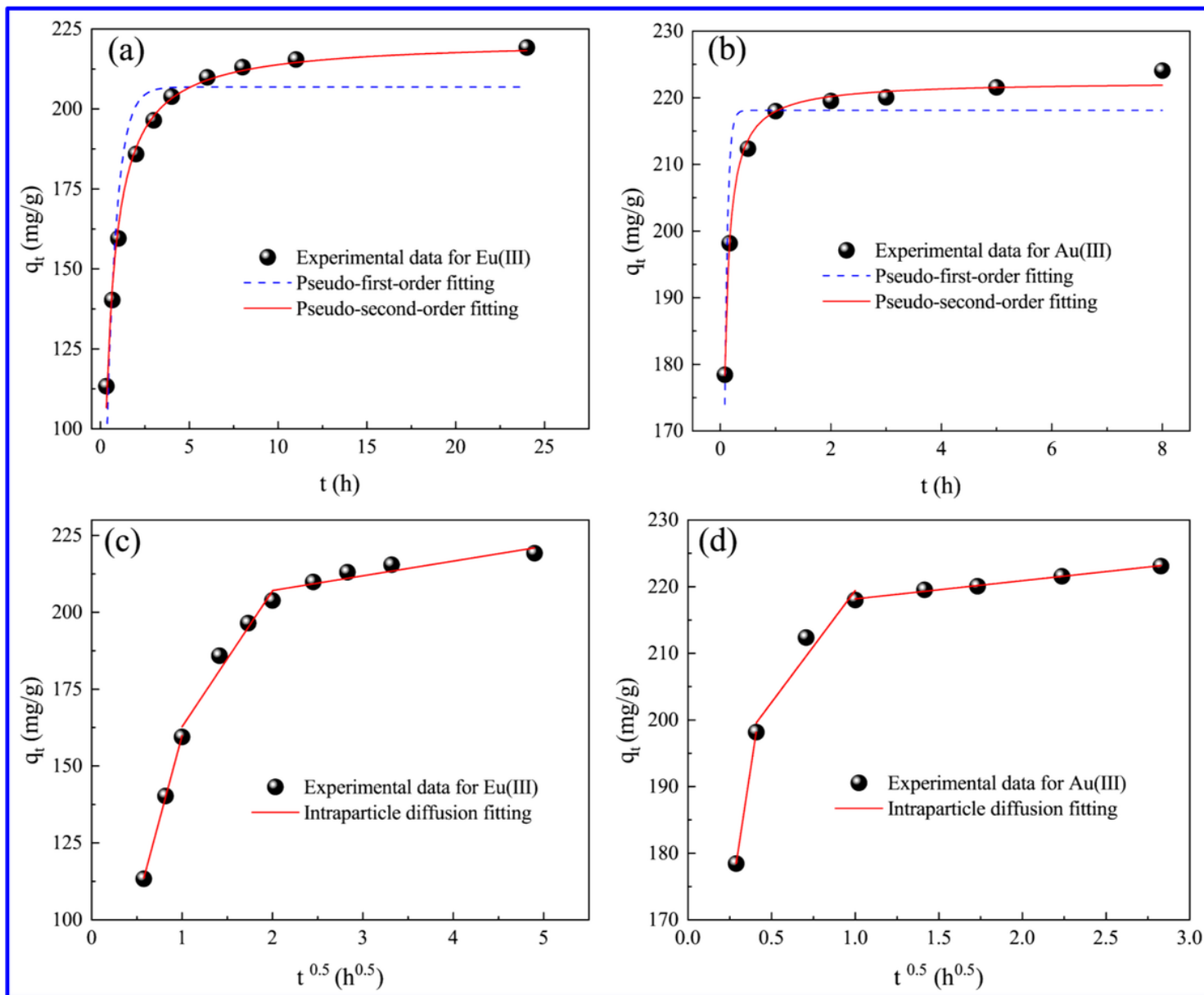


**Figure 6**

Effects of the equilibrium time on Eu(III) and Au(III) adsorbed on DAWP-PEI-β-CD as well as modeling by different kinetics equations.

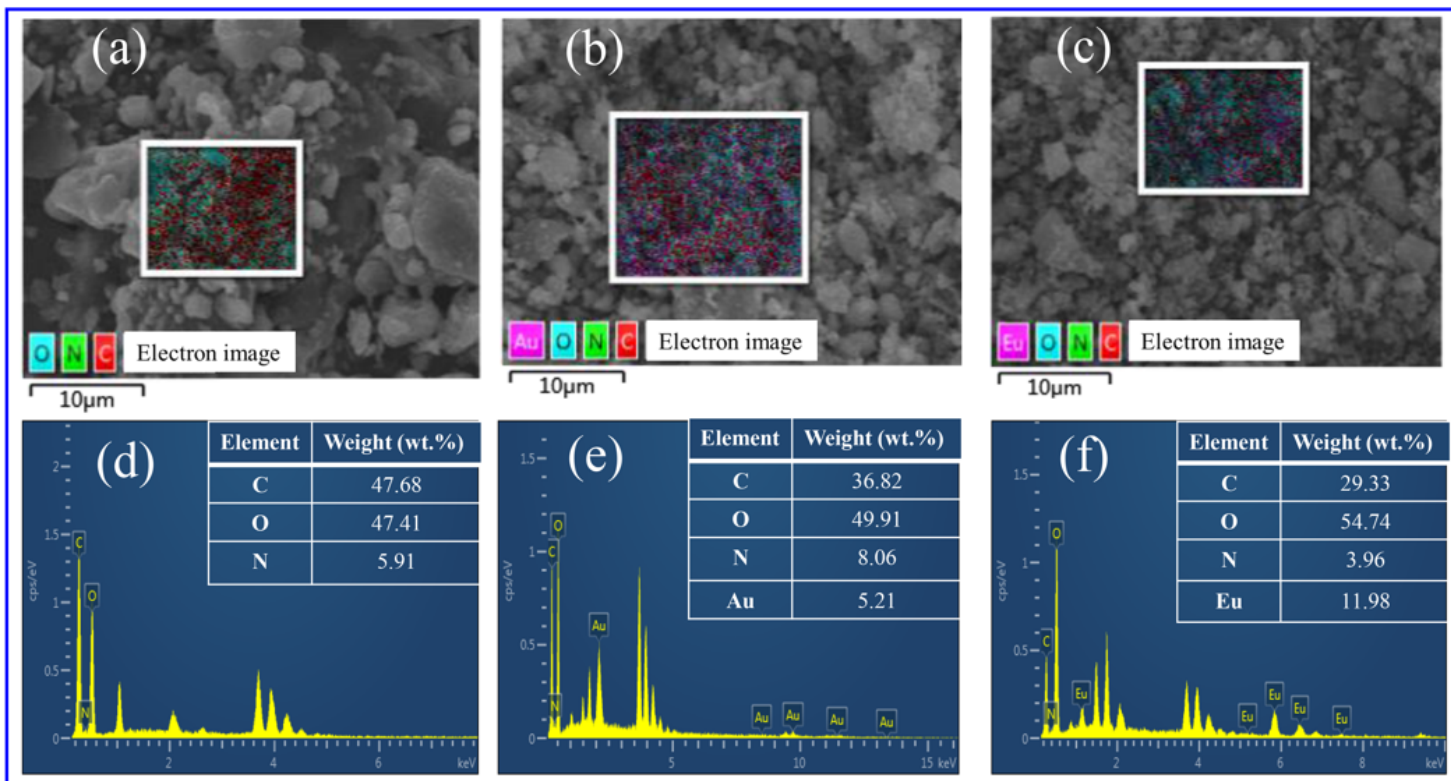


**Figure 7**

The SEM images and EDS spectrum of DAWP-PEI-β-CD (a, d), DAWP-PEI-β-CD-Au (b, e), DAWP-PEI-β-CD-Eu (c, f).

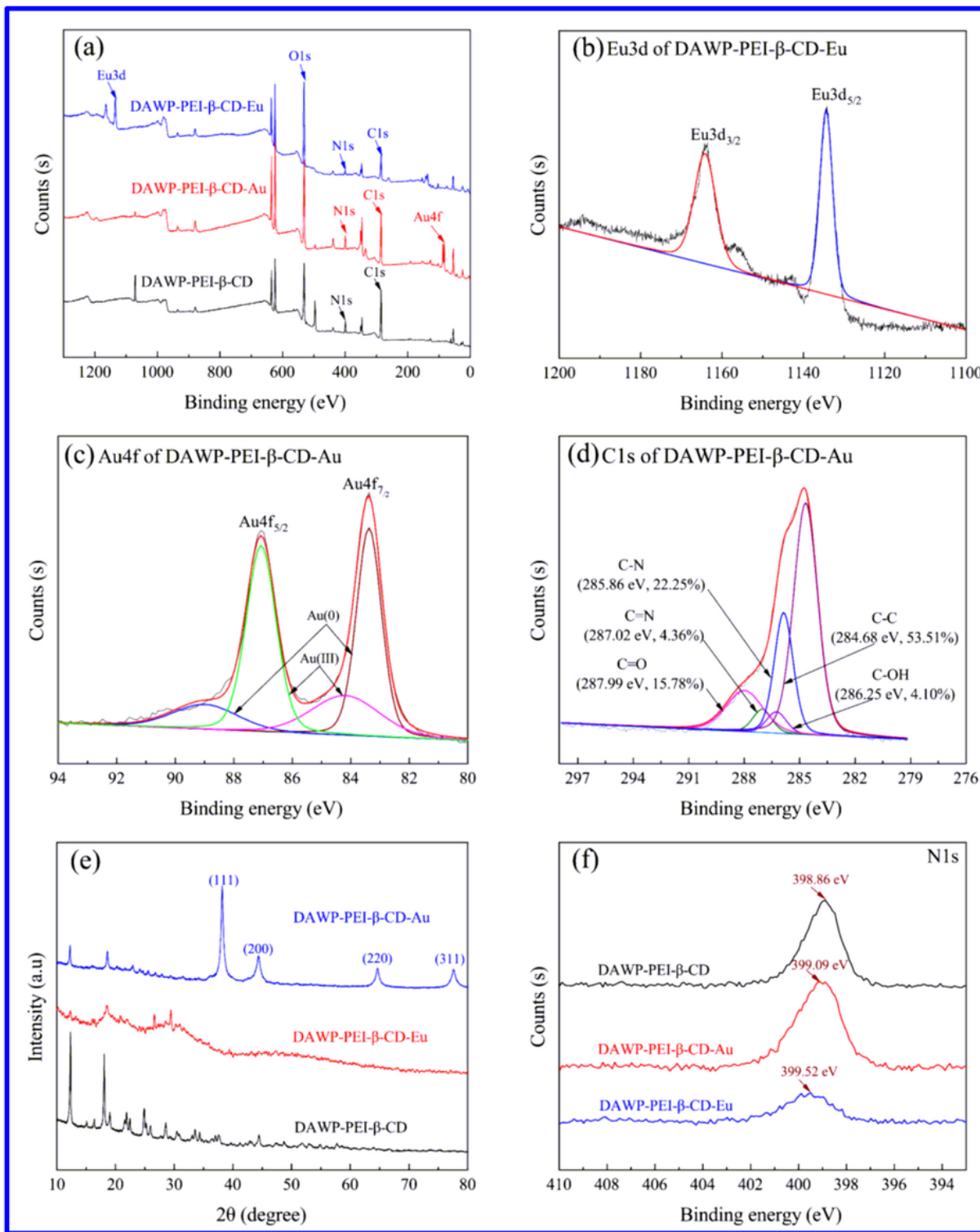


**Figure 8**

XPS survey (a), Eu3d, Au4f, C1s, N1s spectra (b, c, f) and XRD patterns (e) of DAWP-PEI-β-CD, DAWP-PEI-β-CD-Au, DAWP-PEI-β-CD-Eu.

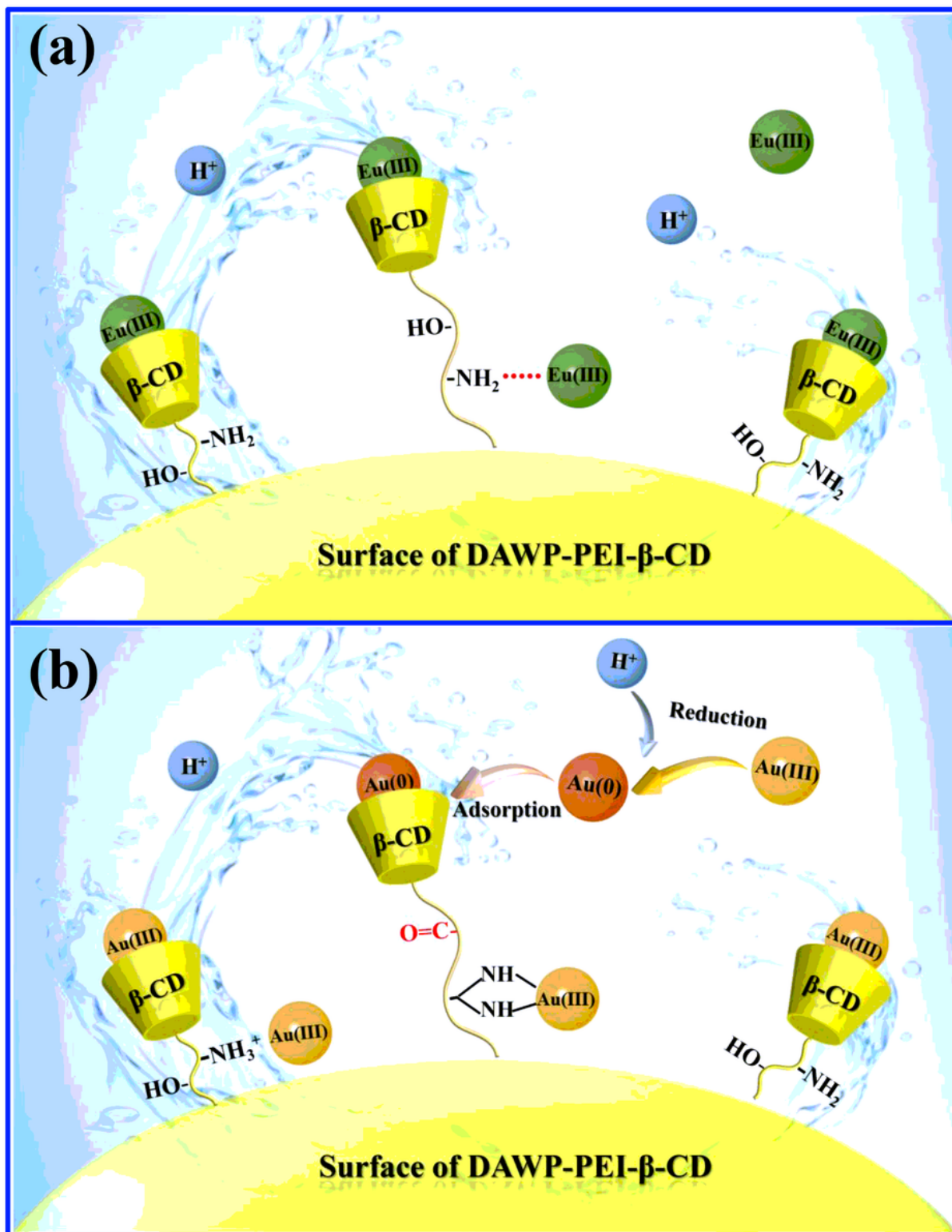


Figure 9

Schematic diagram of the plausible adsorption mechanism of Eu(III) and Au(III) by DAWP-PEI- $\beta$ -CD.

## Supplementary Files

This is a list of supplementary files associated with this preprint. Click to download.

- [GraphicalAbstract.png](#)
- [SupportingMaterials.docx](#)